LUNAR DUST TRANSPORT FROM ROVER WHEEL INTERACTIONS: MODELLING CHARGED DUST GRAINS IN SURFACE ELECTRIC FIELDS. H. M. Sargeant[1], J. Dyson[2], H. Otto[3], J. Long-Fox[1], D. Britt[1], and S. Sheridan[4]. [1]The University of Central Florida (HannahMarie.Sargeant@ucf.edu), [2]The University of Leicester, [3]Engineerdo, [4]The Open University.

Introduction: The uppermost portion of the lunar crust is a regolith layer which can reach depths of up to 20 m on top of which is a very fine, dusty layer about 20 cm thick [1]. The majority of the regolith is defined as lunar soil which is the < 1 cm fraction, where approximately 50 wt % of lunar soil is finer than 50 µm [2]. Soil grains are irregular in shape and have a high surface area, resulting in increased physical adherence to objects and other grains. Lunar soil is also highly cohesive, a result dominated by van der Waals forces and electrostatic interactions (which dominate for the smaller grain sizes of < 1.25 mm) [3], emphasized by the vacuum environment on the Moon and the insulating nature of lunar soil [4]. These jagged, charged grains can cause serious mechanical and electrical problems for lunar surface rovers and instruments.

To effectively mitigate against the damaging effects of lunar soils, their behavior in the lunar environment and the methods of mobilization from the lunar surface must be understood. Dust is known to be mobilized via natural mechanisms such as meteorite impacts and interactions with surface electric fields induced by incident solar plasma. However, these mechanisms are minor compared to the dust transport induced by human activities including spacecraft landing and launch, and rover operations [4].

Here we consider the dust transport from rover operations on the lunar surface and consider if and how the local charging environment may affect the motion of the dust clouds that are produced. We have developed a Discrete Element Method (DEM) simulation to carry out this work.

Lunar charging environment: The lunar surface is subject to the solar wind plasma, and ultraviolet and soft x-ray radiation that can vary over the course of a lunar day [5]. A surface potential is produced on the scale of meters to kilometers above the lunar surface resulting in an induced electric field. Charged dust grains can interact with the surface electric field, affecting the grains' motion. The lunar dayside experiences a surface potential, φ_s, of ~+18 V with a Debye length, λ_D, of ~1 m [6,7], while the lunar night side experiences a φ_s of ~-100 V with a λ_D, of ~1000 m [6,8]. These potentials can become increasingly negative in the hundreds of volts when in the Earth's magnetotail plasma sheath.

The incident solar plasma also provides individual dust grains with a charge, however, when dust is mobilized the dominant source of dust charging is from tribocharging between grains. For example, as wheels move across the lunar surface and dust clouds are produced, the dust grains exchange charge each time they come into contact with each other. Triboelectric charging results in surface potentials on lunar simulant grains in the range of -0.32 ± 2.38 V for 50 µm radius grains [9].

LRV wheels: The dust clouds produced from the Apollo 16 Lunar Roving Vehicle (LRV) traverses were captured on video footage (Fig. 1). At ground speeds of ~2.5 ms^{-1}, a characteristic 'rooster tail' can be seen. It is not fully known how the rover wheel design, rover speed, or environmental conditions may affect the produced dust cloud. We will simulate the conditions of the Apollo 16 Grand Prix traverse using DEM, with a focus on the dust-wheel interactions, to try and replicate the results seen in the footage. This will act as a validation exercise for the model which can then be applied to other wheel designs and environmental conditions.

The LRV wheel design is complex, consisting of a flexible, wire-mesh carcass and a stiff inner frame [10]. We use a simplified LRV CAD design to reduce computational time in our simulations (Fig. 2).

Figure 1 Example rooster tail dust cloud formation during Apollo 16 Grand Prix EVA (credit: NASA).

Figure 2 Left- LRV front fender and wheel replicas (credit: Smithsonian https://airandspace.si.edu/collection-objects/wheel-lunar-rover/nasm_A19750830000). Right- LRV rear fender and wheel CAD.

Simulation conditions: A DEM simulation of an LRV wheel interacting with the lunar surface is in development. The wheel and fender CAD design are integrated into a simulated lunar surface environment using LIGGGHTS [11], an open source DEM particle simulation software. The properties of most interest to this work are the grain sizes and charges, and the electric field present at different times of day on the lunar surface. The behavior of the lunar dust particles are then analyzed following their interaction with the moving rover wheel.

To simply represent the range of grain sizes found in lunar soils, three discrete grain size diameters, *d*, are used in the simulation: 0.469 mm, 0.055 mm, and 0.012 mm (Table 1). The grain sizes and quantity of particles used in the simulation are derived from analyses of the average lunar soil grain size distribution [2]. Using the maximum surface potentials obtained by [9], with the formula for calculating charge, q ($q=2\pi\varepsilon_o d\varphi_s$), the charge of simulated dust grains is calculated (Table 1). Triboelectric charging results in an approximately even distribution of positively and negatively charged grains, therefore the simulated grains will have an equal number of positive and negative charges.

Table 1 Lunar soil properties used in simulation (assuming a rock density of 3365 kg m^{-3} [12].

Grain size (mm), d	Ratio of total mass (wt %), R_{mass}	Mass of grain (kg), m	Triboelectric charge (C), φ_s	
0.469	38	1.82 E^{-7}	+5.37 E^{-14}	-7.04 E^{-14}
0.055	32	2.99 E^{-10}	+6.30 E^{-15}	-8.26 E^{-15}
0.012	30	3.31 E^{-12}	+1.38 E^{-15}	-1.80 E^{-15}

Upon initiation of the simulation, a tray is partially filled with particles with properties shown in Table 1. To reduce simulation time, the particles are all given a fixed triboelectric charge under the assumption that any grains that are mobilized will have a triboelectric charge. A day-side E-field of 18 V up to a height of 1 m is applied above the particles. The simulated wheel and fender are lowered into the tray to a depth estimated from the Apollo 16 footage. Finally the wheel is rolled along the tray and particle trajectory and velocity are recorded (e.g. Fig. 3). Preliminary results of the simulation with the LRV wheel will be presented with comparisons to the Apollo 16 Grand Prix traverse footage.

Applications: Once initial validation with LRV footage is completed, the simulation can be used to understand the effects of other surface charging conditions on dust transport. For example, we will consider whether dust cloud volume or velocity vary significantly when operating rovers during the lunar night, across the terminator, or in a Permanently Shadowed Region (PSR). We can also test future lunar rover wheel and fender designs and wheel speeds to minimize dust transport or protect sensitive instruments.

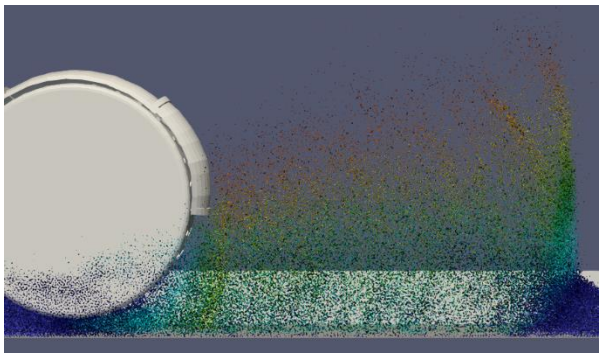

Figure 3 Example simulation output.

Conclusions: Lunar dust becomes mobilized and triboelectrically charged when disturbed by rover wheels. The charged dust can therefore interact with the E-field at the lunar surface. We have developed a DEM simulation of the lunar surface which can be used to model rover wheel-dust interactions and dust mobilization. The simulation can be used to help understand the effects of different E-fields, rover wheel designs, and rover operational scenarios to mitigate against unwanted dust deposits.

Acknowledgements: We thank Ron Creel for providing CAD files and information on the LRV wheels and fenders. This work was initiated as part of the LUVMI-X project which is co-funded by the European Commision through its Horizon 2020 programme under grant agreement #822018. The continuation of this work is supported by CLASS under NASA cooperative agreement #80NSSC19M0214.

References: [1] McKay et al., 1991, *The Lunar Regolith*, in, *The Lunar Sourcebook*, pp. 285-356. [2] Zeng et al., 2010, *Jour. of Aero. Eng*., 23(4), pp. 213-218. [3] Jackson et al., 2015, *Adv. In Space Res*., 55(6), pp.1710-1720. [4] Katzan and Edwards, 1991, Lunar Dust Transport and Potential Interactions With Power System Components, NASA contractor report #4404. [5] Manka, 1973, *Photon and Particle Interactions with Surfaces in Space, Proc. Of the 6th ESLAB Symp*. 37, pp. 347-361. [6] Freeman & Ibrahim, 1975, *The Moon*, 14 (1), pp. 103-114. [7] Stubbs et al., 2006, *Adv. In Space Res.*, 37(1), pp.59-66. [8] Halekas, 2003, *Geophys. Res. Let.*, 20(21) pp. 2117. [9] Sickafoose et al., 2001, *Jour. of Geophys. Res.: Space. Phys.*, 106 (A5), pp. 8343-8356. [10] Asnani et al., 2009, The development of Wheels for the Lunar Roving Vehicle, NASA/TM-2009-215798. [11] CFDEM Project, 2021, LIGGGHTS, https://www.cfdem.com/liggghtsr-open-source-discrete-element-method-particle-simulation-code. [12] Kiefer et al., 2012, *Geophys. Res. Let.*, 39(7) pp.1-5.